

# **Supplement to 'The contribution of transport emissions to ozone mixing ratios and methane lifetime in 2015 and 2050 in the Shared Socioeconomic Pathways (SSPs)'**

Mariano Mertens et al.  
Institut für Physik der Atmosphäre  
DLR-Oberpfaffenhofen

`mariano.mertens@dlr.de`

August, 2024

## S1 Emissions

Figures S1–S3 display the annual average  $\text{NO}_x$  flux for all consider emission cases for the sectors shipping, land transport and aviation. Tables S1–S3 list the global total emissions of  $\text{NO}_x$ , CO and NMHC.

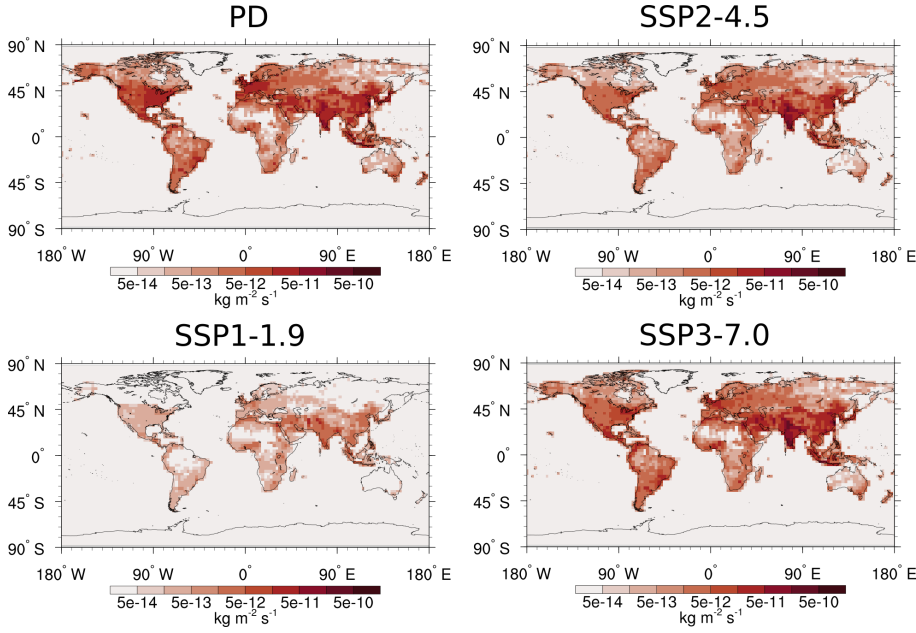


Figure S1: Annual average flux of  $\text{NO}_x$  emissions from land transport in  $\text{kg (NO)}\text{m}^{-2}\text{s}^{-1}$  for *PD*, *SSP1-1.9*, *SSP2-4.5* and *SSP3-7.0*.

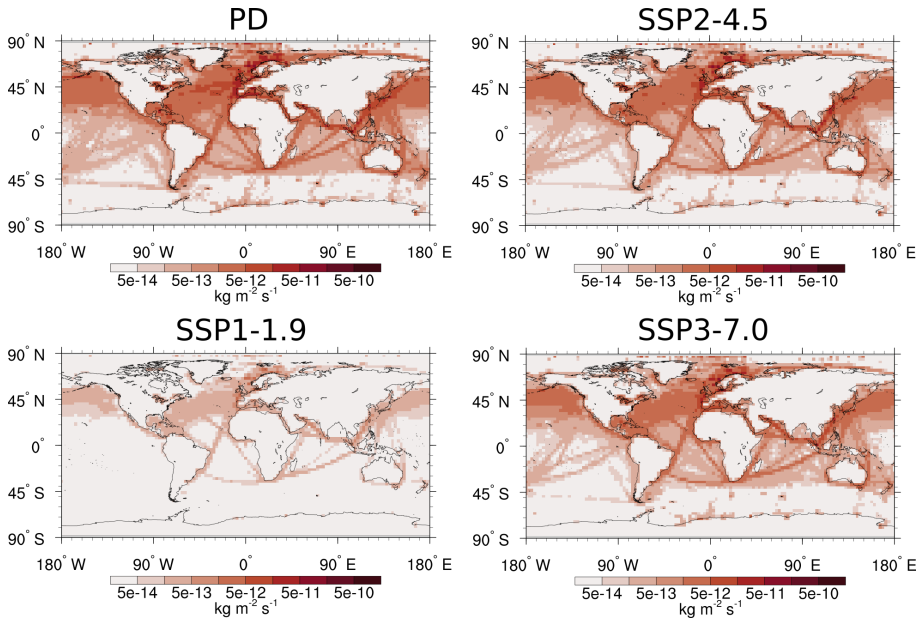


Figure S2: Annual average flux of  $\text{NO}_x$  emissions from shipping in  $\text{kg (NO)}\text{m}^{-2}\text{s}^{-1}$  for *PD*, *SSP1-1.9*, *SSP2-4.5* and *SSP3-7.0*.

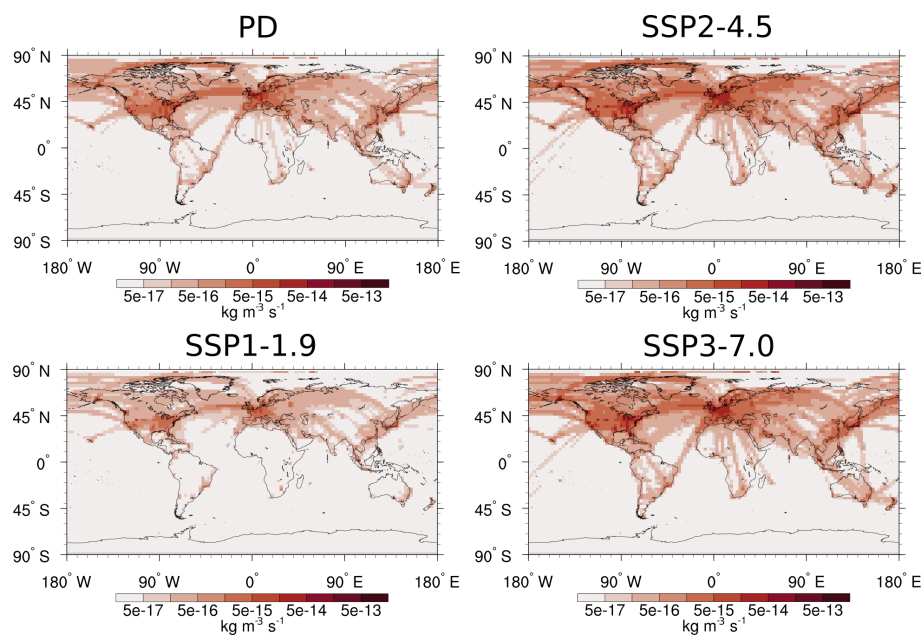


Figure S3: Annual average flux of  $\text{NO}_x$  emissions from aviation in  $\text{kg (NO)}\text{m}^{-3}\text{s}^{-1}$  for *PD*, *SSP1-1.9*, *SSP2-4.5* and *SSP3-7.0*.

Table S1: Total NO<sub>x</sub> emissions of the different emission sectors (in Tg(NO) a<sup>-1</sup>) as applied in the four simulations. Emissions of soil-NO<sub>x</sub> and lightning are averaged for 2013–2017, all other emissions are the same in each year. AWB stands for agricultural waste burning.

	<i>PD</i>	<i>SSP2-4.5</i>	<i>SSP1-1.9</i>	<i>SSP3-7.0</i>
land transport EU	2.96	1.08	0.12	1.78
land transport NA	4.29	1.15	0.08	2.21
land transport SA	5.80	9.39	0.79	11.27
land transport EA	6.64	3.68	0.35	6.51
land transport ROW	9.30	6.25	1.16	12.93
shipping	15.43	11.38	0.78	8.66
aviation	2.04	4.22	0.74	3.79
anthropogenic non-traffic EU	3.57	2.49	1.44	2.73
anthropogenic non-traffic NA	4.02	2.03	1.23	3.03
anthropogenic non-traffic SA	7.63	7.42	4.57	11.04
anthropogenic non-traffic EA	18.33	8.19	4.86	22.78
anthropogenic non-traffic ROW	15.08	13.02	8.92	18.77
AWB	1.10	0.97	1.71	1.97
biogenic	13.02	13.02	13.02	13.02
biomass burning	12.90	11.10	10.24	10.60
lightning	9.83	9.83	9.83	9.83

Table S2: Total CO emissions of the different emission sectors (in Tg(CO) a<sup>-1</sup>) as applied in the four simulations.

	<i>PD</i>	<i>SSP2-4.5</i>	<i>SSP1-1.9</i>	<i>SSP3-7.0</i>
land transport EU	7.26	5.77	1.14	5.01
land transport NA	24.67	15.87	1.14	22.90
land transport SA	17.39	24.43	2.04	21.26
land transport EA	24.05	31.26	10.26	21.60
land transport ROW	75.73	56.93	7.21	80.69
shipping	0.72	0.40	0.42	0.60
aviation	0.57	1.01	0.58	1.08
anthropogenic non-traffic EU	20.34	9.45	7.48	22.60
anthropogenic non-traffic NA	23.24	14.91	4.47	20.12
anthropogenic non-traffic SA	189.06	90.72	34.53	135.08
anthropogenic non-traffic EA	85.52	84.84	63.64	22.60
anthropogenic non-traffic ROW	155.45	124.57	59.52	181.89
AWB	28.57	25.43	42.792	53.60
biogenic	114.56	114.56	114.56	114.56
biomass burning	304.99	264.68	219.90	275.92



Table S3: Total VOC emissions of the different emission sectors (in  $\text{Tg(C) a}^{-1}$ ) as applied in the four simulations. Emissions of biogenic  $\text{C}_5\text{H}_8$  are averaged for 2013–2017, all other emissions are the same in every year. Please further note, that the emissions of biogenic  $\text{C}_5\text{H}_8$  are scaled with a factor of 0.6 before added to the chemical tracer.

	<i>PD</i>	<i>SSP2-4.5</i>	<i>SSP1-1.9</i>	<i>SSP3-7.0</i>
land transport EU	1.18	0.62	0.07	0.68
land transport NA	0.89	0.93	0.11	1.13
land transport SA	4.57	2.42	0.28	7.47
land transport EA	1.57	5.7	0.70	2.22
land transport ROW	10.75	7.21	0.61	13.69
shipping	2.37	0.34	1.40	1.91
aviation	0.087	0.15	0.034	0.16
anthropogenic non-traffic EU	4.41	3.62	1.55	3.88
anthropogenic non-traffic NA	6.52	4.79	1.02	6.51
anthropogenic non-traffic SA	11.18	10.89	6.26	16.47
anthropogenic non-traffic EA	20.63	19.23	2.88	25.47
anthropogenic non-traffic ROW	4.41	3.62	1.55	3.88
AWB	4.03	3.34	5.99	5.11
biogenic	107.41	107.41	107.41	107.41
biogenic $\text{C}_5\text{H}_8$	524.23	524.23	524.23	524.23
biomass burning	44.23	37.58	31.58	38.98

## S2 Ground-level ozone

Figure S4 shows the ozone ground-level mixing ratios as simulated by *PD*, *SSP1-1.9*, *SSP2-4.5* and *SSP3-7.0*.

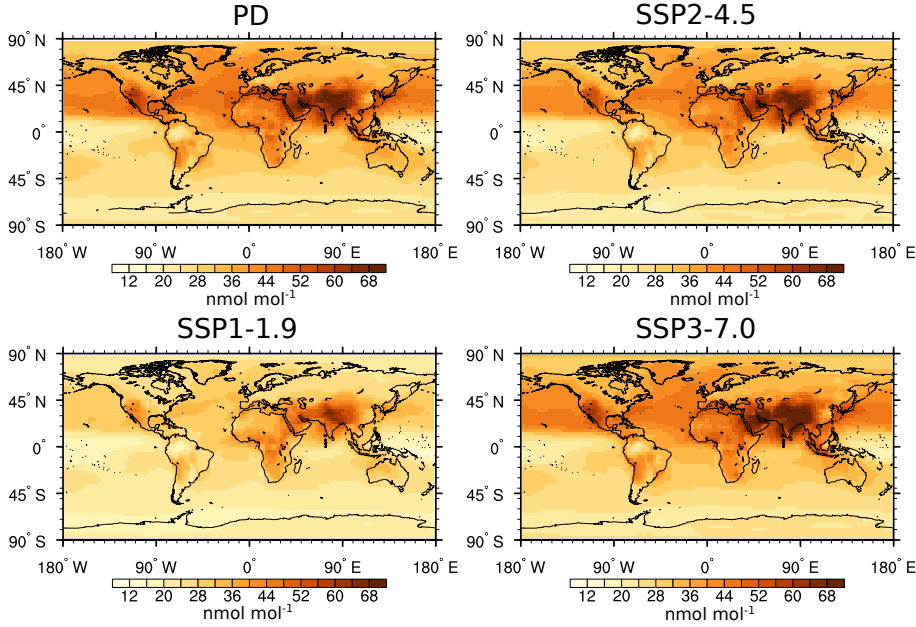


Figure S4: Ozone mixing ratios (in  $\text{nmol mol}^{-1}$ ) at ground-level for *PD*, *SSP1-1.9*, *SSP2-4.5* and *SSP3-7.0*. Shown are 5 year average values.

## S3 Absolute contributions

Figures S5 to S8 display the absolute contributions of land transport emissions to ground-level ozone for the different source regions. Figure S9 show the absolute contribution of shipping emissions to ground-level ozone.

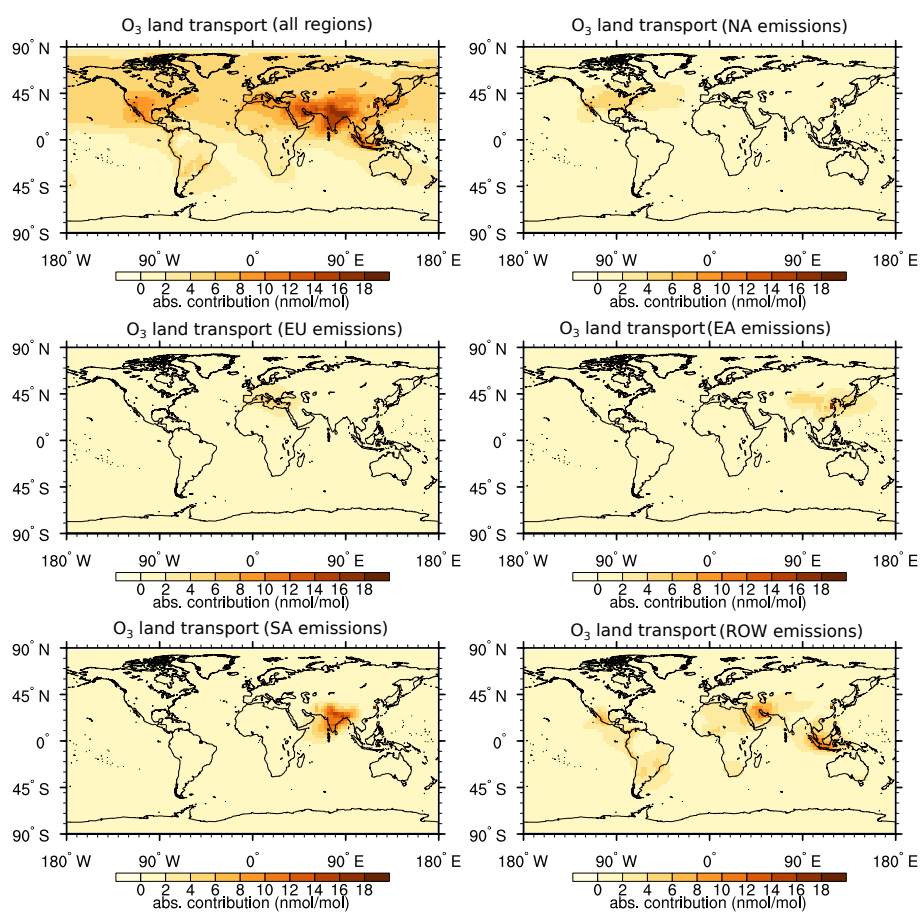


Figure S5: Absolute contributions (5-year average) of land transport emissions (in  $\text{nmol mol}^{-1}$ ) for  $PD$ ; 'all regions' is the sum of the source regions  $NA+EU+EA+SA$  and  $ROW$ . The other figures show the contribution of the land transport emissions from the different regions.

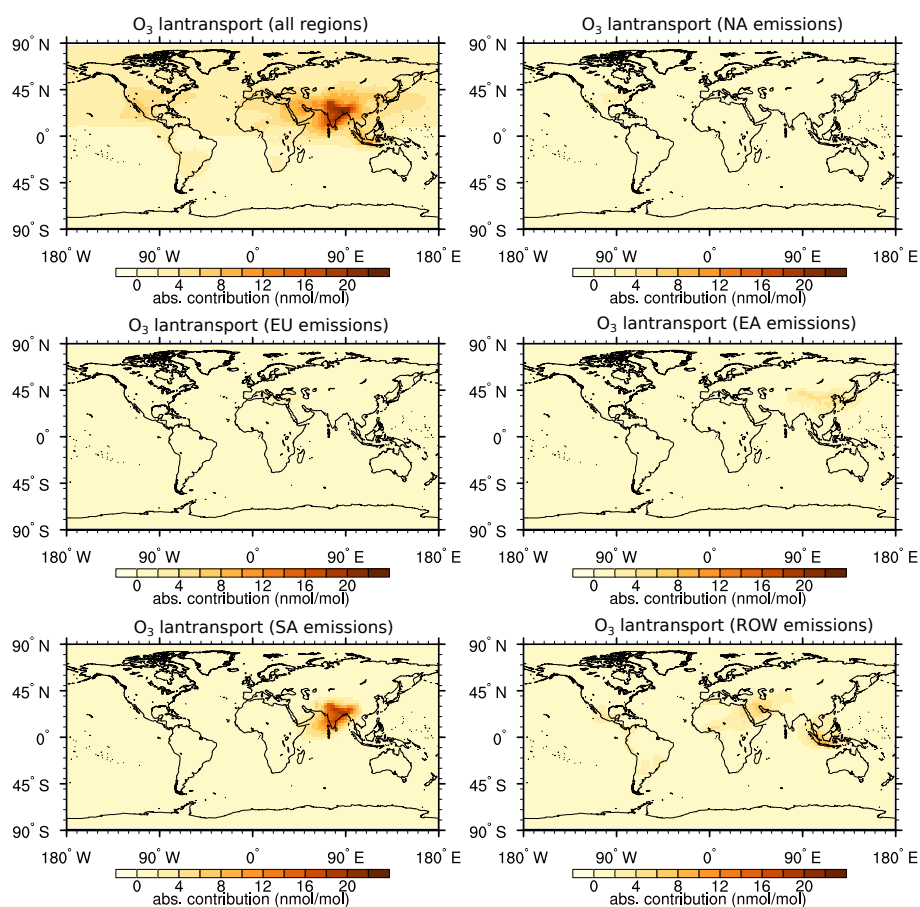


Figure S6: Absolute contributions of land transport emissions (in  $\text{nmol mol}^{-1}$ ) for *SSP2-4.5*; 'all regions' is the sum of the source regions NA+EU+EA+SA and ROW. The other figures show the contribution of the land transport emissions from the different regions.

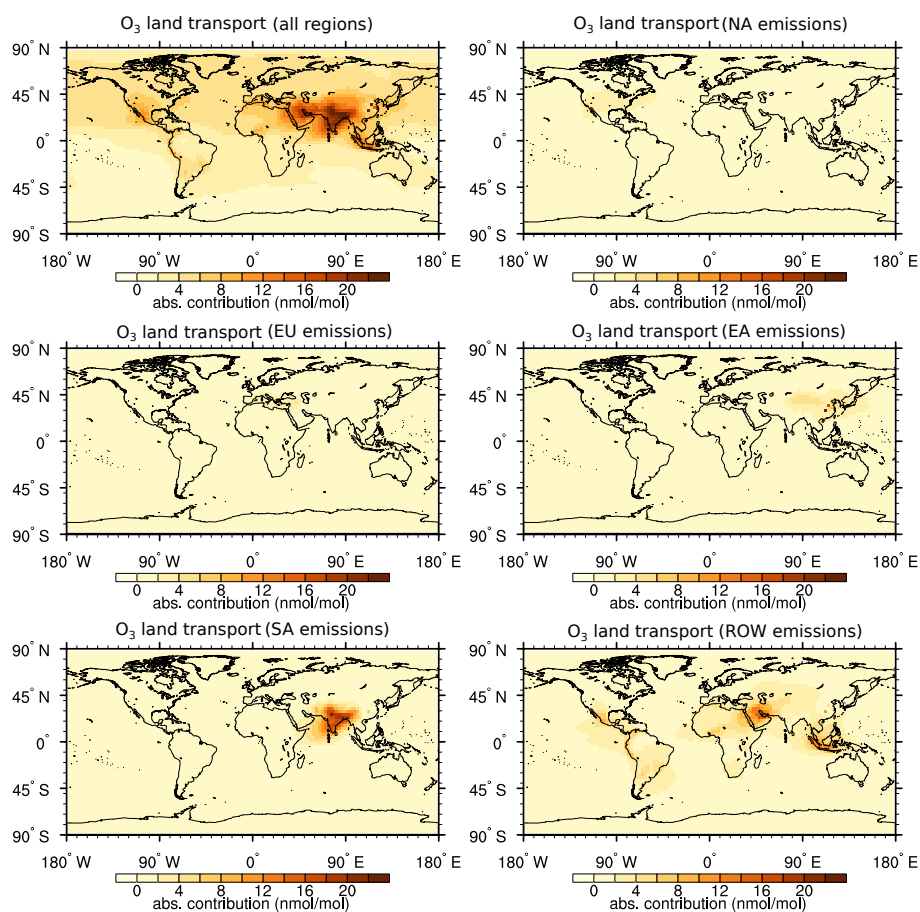


Figure S7: Absolute contributions (5-year average) of land transport emissions (in  $\text{nmol mol}^{-1}$ ) for *SSP3-7.0*; 'all regions' is the sum of the source regions NA+EU+EA+SA and ROW. The other figures show the contribution of the land transport emissions from the different regions.

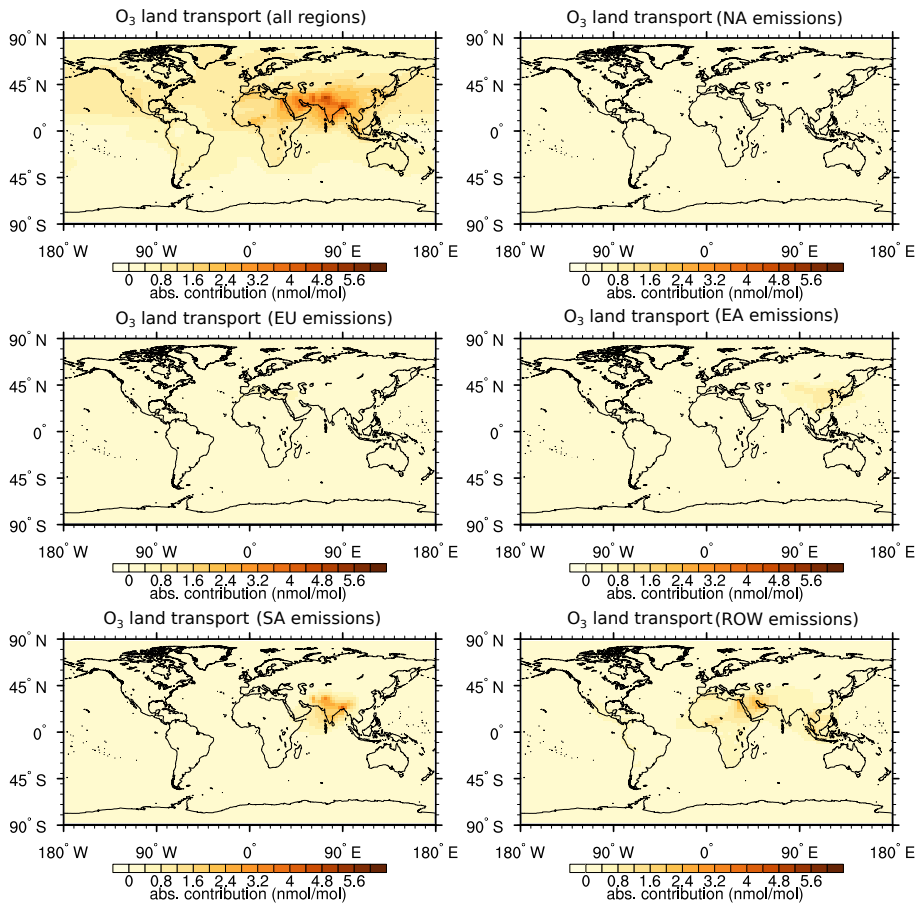


Figure S8: Absolute contributions (5-year average) of land transport emissions (in  $\text{nmol mol}^{-1}$ ) for *SSP1-1.9*; 'all regions' is the sum of the source regions NA+EU+EA+SA and ROW. The other figures show the contribution of the land transport emissions from the different regions.

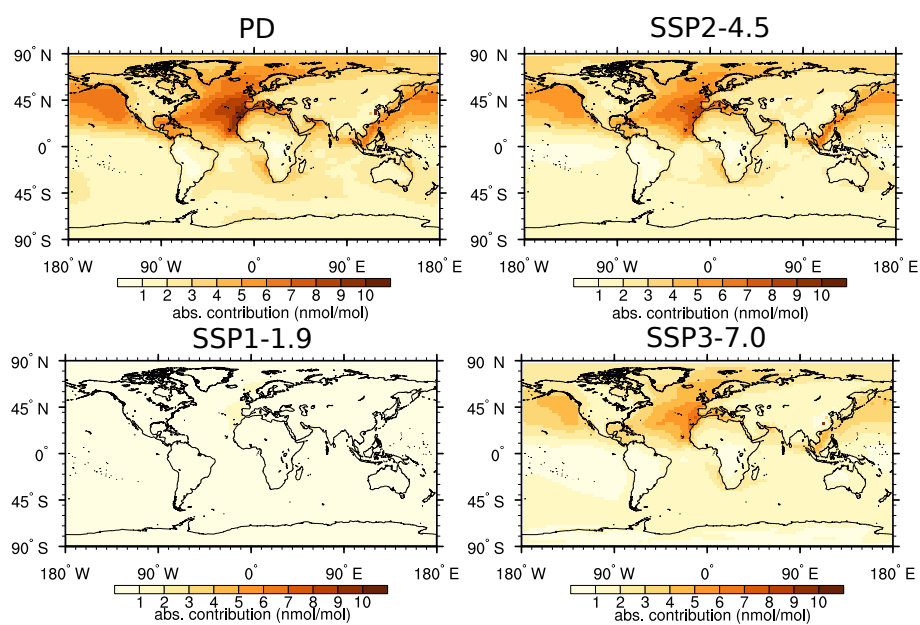


Figure S9: Absolute contributions (5-year average) of shipping emissions to ground-level ozone (in nmol mol<sup>-1</sup>) for *PD*, *SSP2-4.5*, *SSP1-1.9* and *SSP3-7.0*.

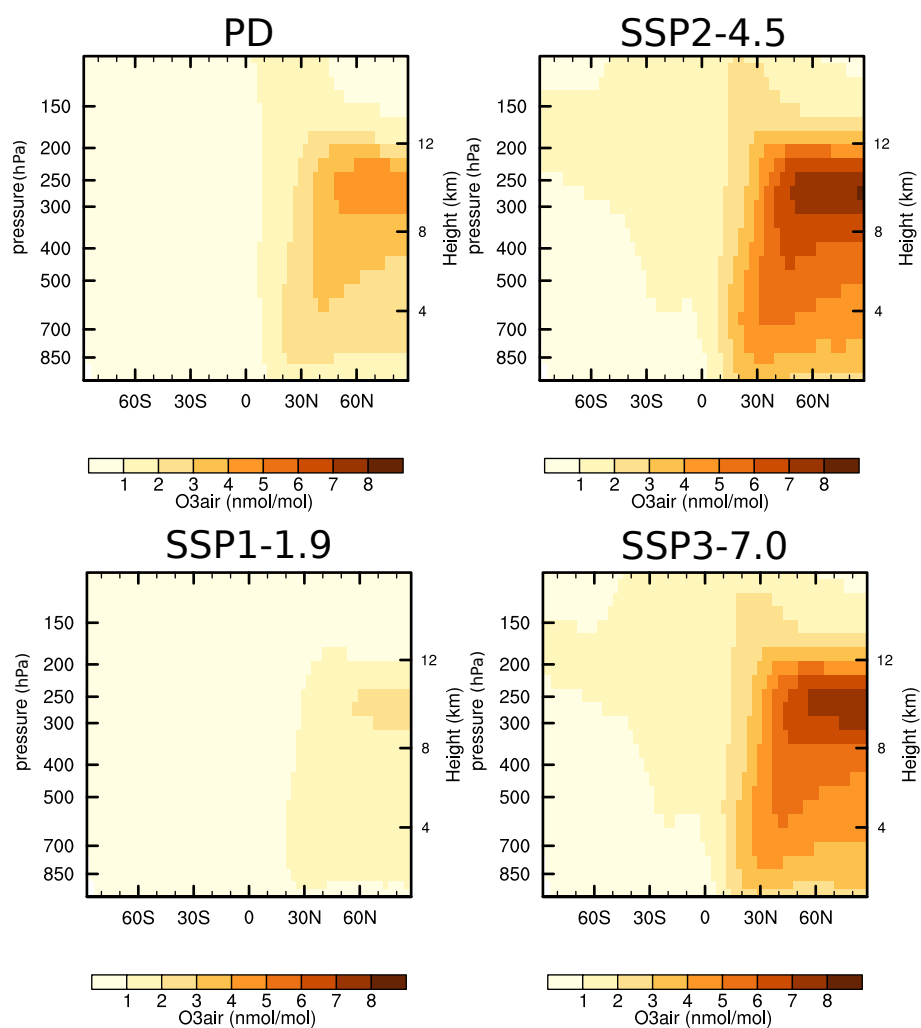


Figure S10: Zonal average of  $O_3^{\text{air}}$  (in  $\text{nmol mol}^{-1}$ ) for *PD*, *SSP2-4.5*, *SSP1-1.9* and *SSP3-7.0*.



## S4 Zonal mean average contributions

### S4.1 Land transport

Figure S11 shows the zonal average of  $C^{\text{tra}}(\text{O}_3)$ .

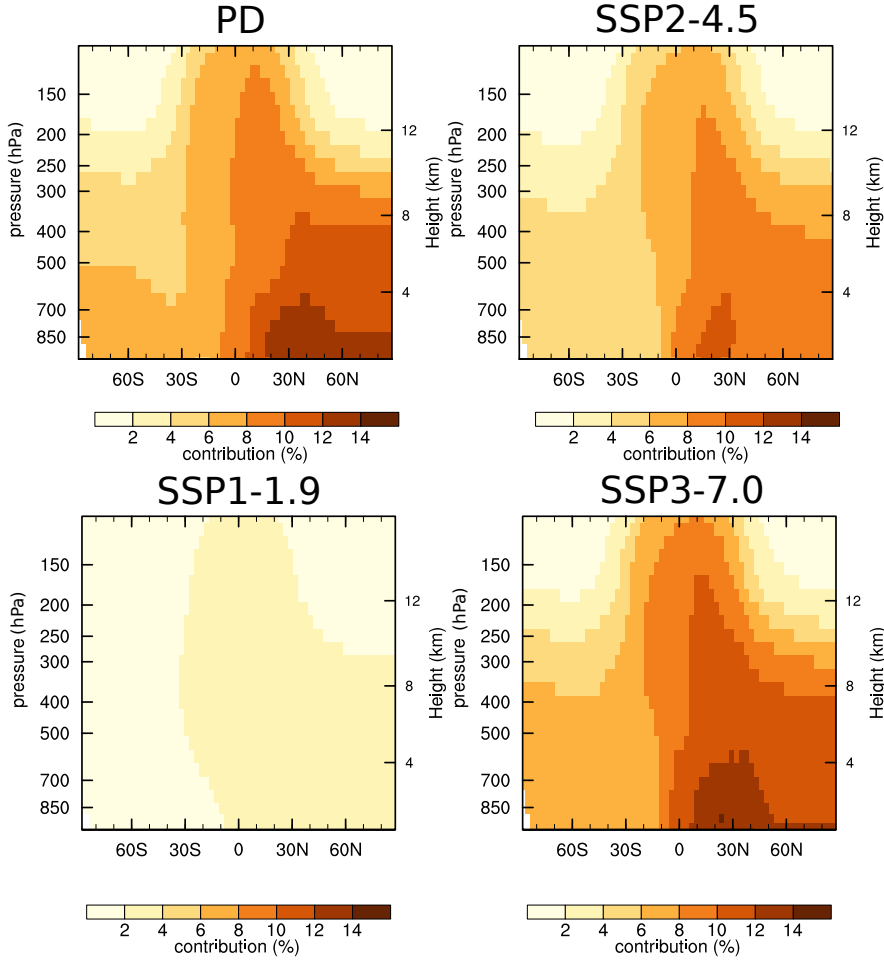


Figure S11: Zonal average of the relative contribution of land transport emissions to ozone (in %) for *PD*, *SSP1-1.9*, *SSP2-4.5* and *SSP3-7.0*. Values are averaged for 5 years.

## S4.2 Shipping

Figure S12 shows the zonal average of  $C^{\text{ship}}(\text{O}_3)$ .

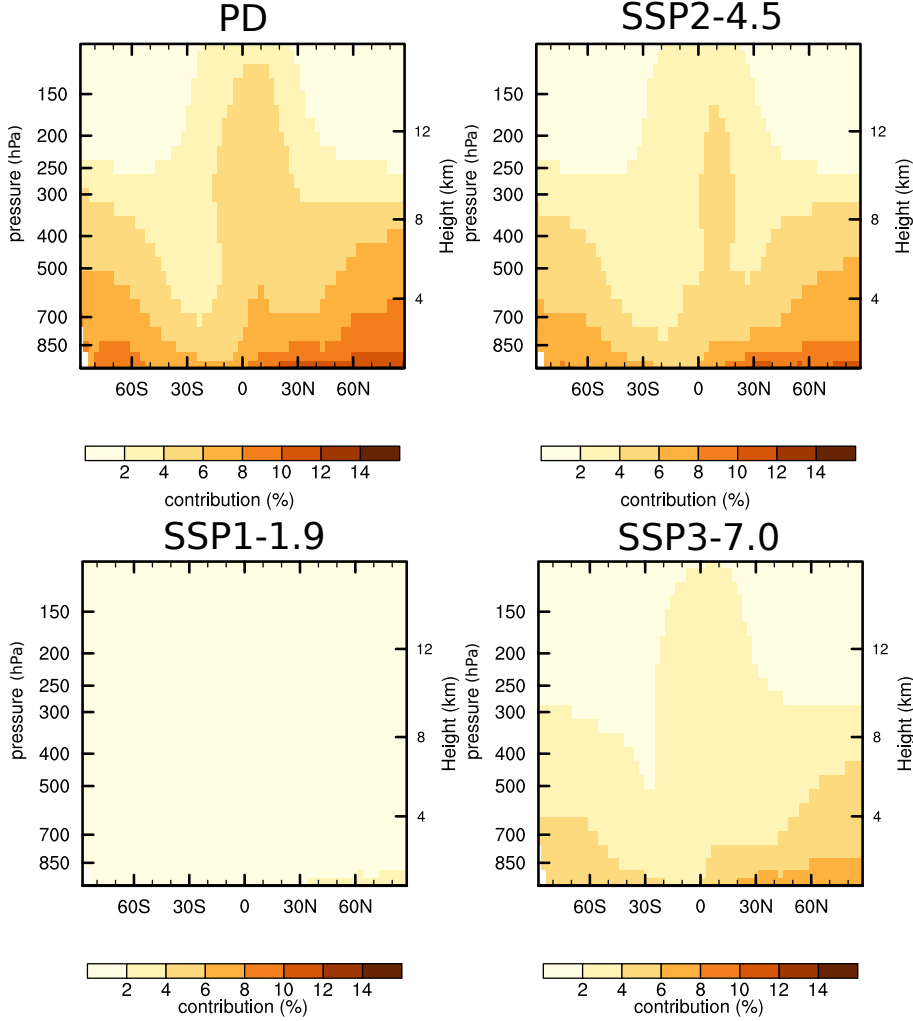


Figure S12: Zonal average of the relative contribution of shipping emissions to ozone (in %) for *PD*, *SSP1-1.9*, *SSP2-4.5* and *SSP3-7.0*. Values are averaged for 5 years.

## S5 Comparison of Tagging and Perturbation approach to quantify reductions of the methane lifetime by specific emissions

Table S4 compares the estimated reductions of the methane lifetime due to emissions from the three transport sectors between the present study and Hoor et al. (2009). Our results obtained with a 5 % perturbation are very similar to the results of the 5 % perturbation of Hoor et al. (2009). Accordingly, the large difference of the reductions on the methane lifetime by the tagging approach and previously reported results can be attributed to the methodological differences.

Table S4: Comparison of methane lifetime changes by transport emissions. All values are given in %. The values for Hoor et al. (2009) and for the 5 % perturbation are scaled to a full perturbation

	this study (5 % perturbation)	Hoor et al. (2009)	this study (tagging)
Land transport	-1.9 %	-1.6 %	-14.3 %
shipping	-4.5 %	-4.1 %	-8.5 %
aviation	-1.1 %	-1.0 %	-3.8 %

## S6 Sensitivity simulation with increased methane levels

Table S5 lists the tropospheric ozone columns of all tagged categories for the *SSP2-4.5* simulation and a simulation with the same emissions as *SSP2-4.5* and additionally increased methane levels according to 2050 conditions. This leads to an increase of methane by around 9 %.

Table S5: Global 5-year average tropospheric ozone columns (in DU) of all tagged categories for the *SSP2-4.5* simulation and a simulation with increase methane levels. See Table 1 in the manuscript for a detailed description of the abbreviations.

	<i>SSP2-4.5</i>	<i>SSP2-4.5</i> with increased methane	change in %
LT-ROW	1.02	1.03	1.3
LT-EU	0.19	0.19	1.8
LT-NA	0.24	0.25	2.4
LT-SA	0.71	0.72	1.5
total land transport	2.59	2.62	1.1
IN-ROW	2.72	2.74	0.8
IN-EU	0.32	0.32	1.4
IN-EA	1.09	1.10	0.1
IN-SA	0.84	0.83	-0.8
IN-NA	0.42	0.42	0.4
total anth. non-traf.	5.38	5.41	0.4
SHP	1.49	1.5	2.4
LIG	6.44	6.7	3.7
BB	1.90	1.9	0.8
SOIL	5.34	5.3	-0.4
AIR	1.48	1.5	2.9
N <sub>2</sub> O	0.78	0.81	3.1
CH <sub>4</sub>	5.40	5.90	9.1
stratosphere	5.59	5.611	0.5

## S7 Analysis of the non-linearity of the OH chemistry

To analyse how the OH burden efficiency changes for the different projections, we introduce the following metric exemplarily for the shipping sector:

$$\chi_{OH}^{SHP} = \frac{B(OH^{SHP})}{E(NO_x^{SHP})}. \quad (1)$$

In this definition,  $B(OH^{SHP})$  is the global burden (in Tg) of  $OH^{SHP}$  and  $E(NO_x^{SHP})$  are the annual  $NO_x$  emissions of the shipping sector in Tg(NO). Increasing values of  $\chi_{OH}$  indicate an increase of the ozone burden efficiency.

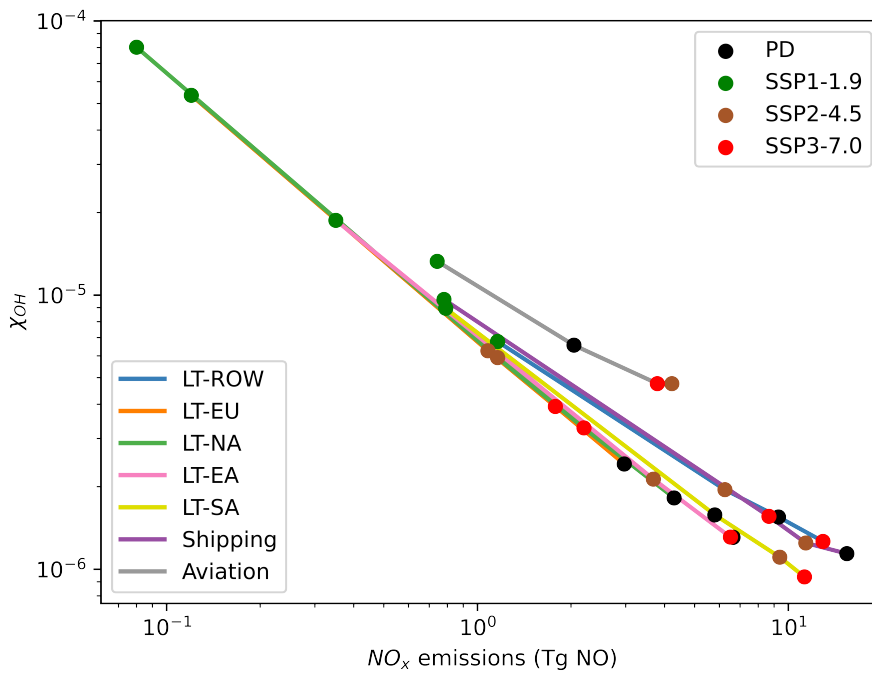


Figure S13: Dependency between  $\chi_{OH}$  and the annual  $NO_x$  emissions (in Tg(NO)).  $\chi_{OH}$  is calculated as global mean over 5 years. Shown are the results of the 7 transport categories (land transport (indicated as LT-): ROW, EU, NA, SA and EA, aviation and shipping) for each simulation (colour coded).

## S8 Definitions of source regions

Figure S14 displays the used source regions for the TAGGING method.

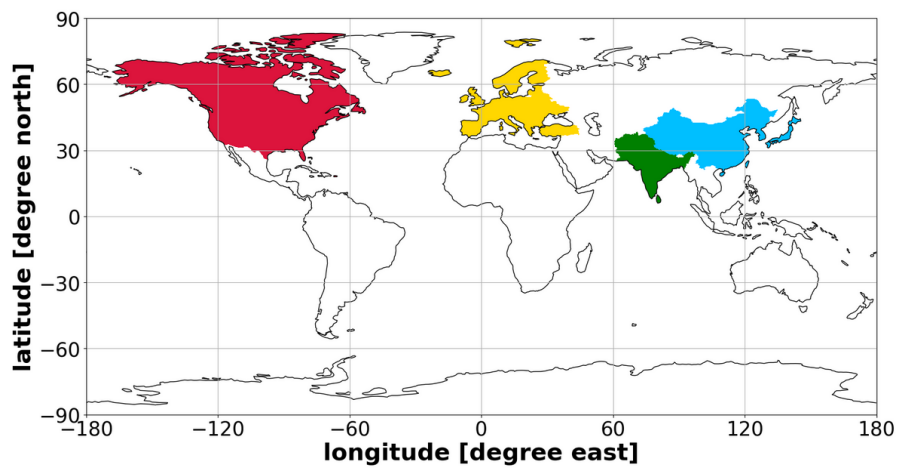


Figure S14: Definitions of the 5 source regions; (red) North America, (yellow) Europe, (green) South Asia, (light blue) East Asia, (white) rest of the world.

## S9 Definitions of analyses regions

### S9.1 Land transport

We define the analyses regions as rectangular regions as follows:

- Europe:  $30^{\circ} : 70^{\circ}$  N ;  $-15^{\circ} : 50^{\circ}$  E
- North America:  $15^{\circ} : 55^{\circ}$  N ;  $-130^{\circ} : -60^{\circ}$  E
- South America:  $15^{\circ}$  N ;  $-55^{\circ}$  S ;  $-85^{\circ} : -30^{\circ}$  E
- East Asia:  $18^{\circ} : 55^{\circ}$  N ;  $90^{\circ} : 150^{\circ}$  E
- South Asia:  $5^{\circ} : 35^{\circ}$  N ;  $65^{\circ} : 95^{\circ}$  E
- South East Asia:  $-12^{\circ} : 25^{\circ}$  N ;  $95^{\circ} : 140^{\circ}$  E

### S9.2 Shipping

We define the analyses regions as rectangular regions as follows:

- Atlantic Ocean:  $15^{\circ} : 60^{\circ}$  N ;  $-80^{\circ} : -10^{\circ}$  E
- Indian Ocean:  $-30^{\circ} : 20^{\circ}$  N ;  $40^{\circ} : 115^{\circ}$  E
- Pacific:  $15^{\circ} : 60^{\circ}$  N ;  $40^{\circ} : -115^{\circ}$  E
- Mediterranean:  $32^{\circ} : 44^{\circ}$  N ;  $-15^{\circ} : 30^{\circ}$  E

### S9.3 Aviation

We define the analyses regions as rectangular regions as follows:

- EUASIA:  $-10^{\circ} : 60^{\circ}$  N ;  $5^{\circ} : 120^{\circ}$  E
- USASIA:  $20^{\circ} : 70^{\circ}$  N ;  $110^{\circ} : -95^{\circ}$  E
- USAEU:  $30^{\circ} : 60^{\circ}$  N ;  $-100^{\circ} : 15^{\circ}$  E

## S10 Comparison with RC1SD-base-10a simulation

The results of the *RC1SD-base-10a* have been evaluated extensively by Jöckel et al. (2016). The model set-up used in the current study is very similar to that of the *RC1SD-base-10a*. Besides updates in the model infrastructure and specific bug fixes the main difference between the two simulation set-ups are the emission data. Our *PD* simulation overlaps with the *RC1SD-base-10a* simulation for the years 2013–2014. Therefore, we compare the results of *PD* with the results of *RC1SD-base-10a* for this time period.

Figure S15 shows the absolute and relative difference of ozone between *PD* and *RC1SD-base-10a*. Similar comparisons for OH and  $\text{NO}_x$  are given in Figs. S16 and Figs. S17.

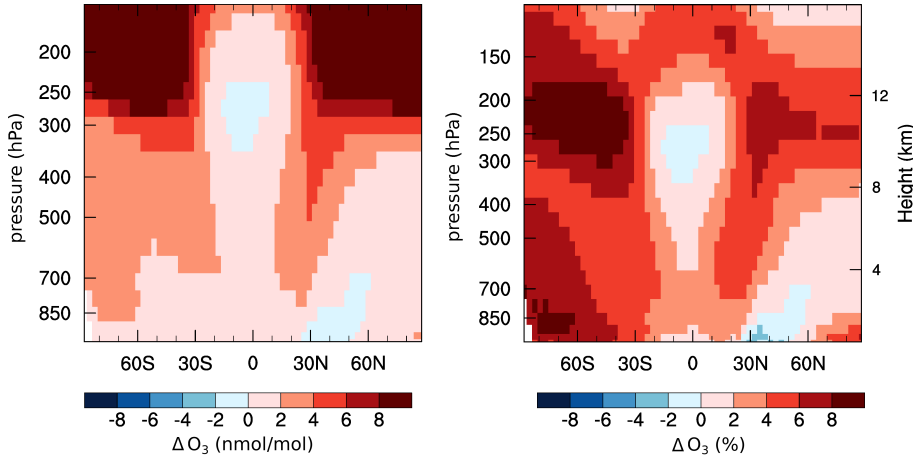


Figure S15: Absolute (left) and relative difference between the zonally averaged ozone mixing ratios of *PD* and the *RC1SD-base-10a* simulation results ('PD MINUS RC1SD-base-10a'). The values are averaged for 2013 and 2014.

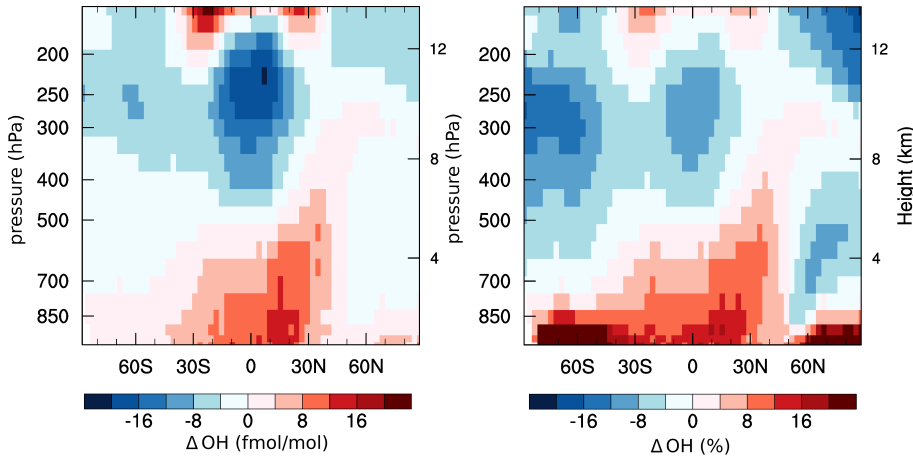


Figure S16: Absolute (left) and relative difference between the zonally averaged OH mixing ratios of *PD* and the *RC1SD-base-10a* simulation results ('PD MINUS RC1SD-base-10a'). The values are averaged for 2013 and 2014.



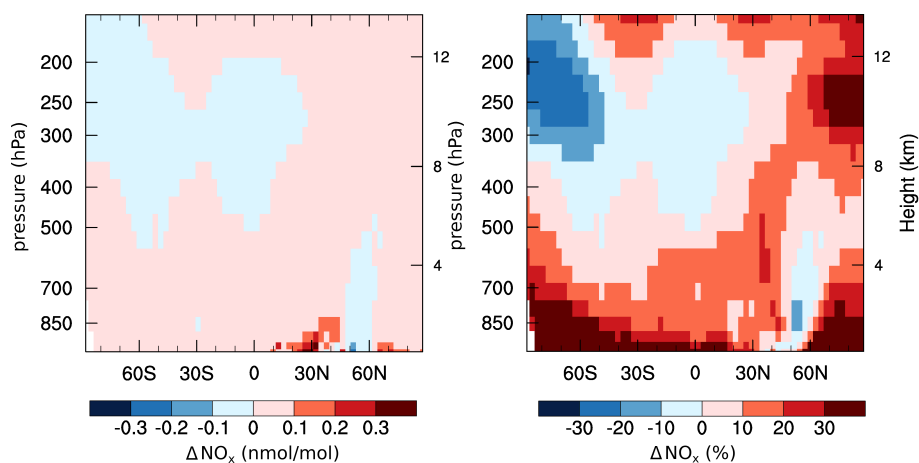


Figure S17: Absolute (left) and relative difference between the zonally averaged NO<sub>x</sub> mixing ratios of *PD* and the *RC1SD-base-10a* simulation results ('PD MINUS RC1SD-base-10a'). The values are averaged for 2013 and 2014.

## S11 Additional figures

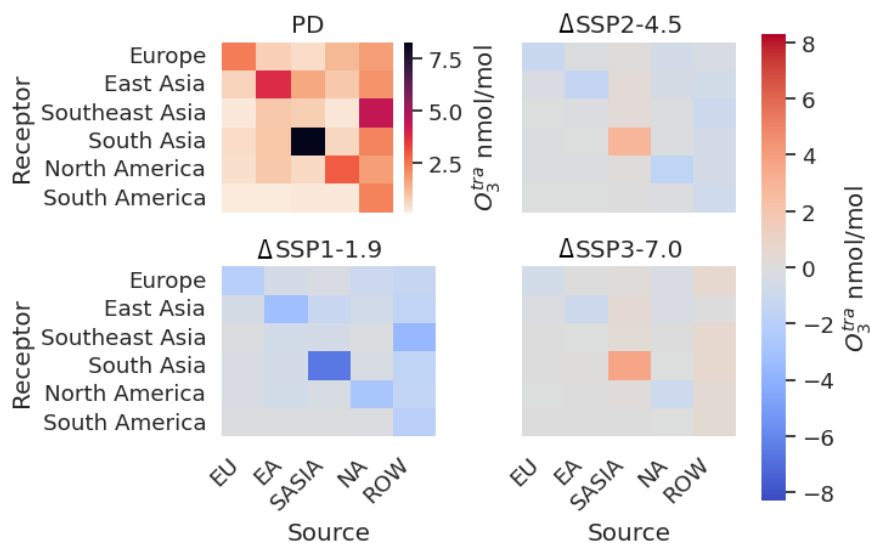


Figure S18: Source receptor analysis of the absolute contribution of land transport emissions to ground-level ozone (in  $\text{nmol mol}^{-1}$ ). The values are mean values over 5 years and area weighted over the receptor regions. Exact definitions of the receptor regions are given in Sect. S9.1 in the Supplement. PD shows the absolute contributions for PD, all other panels show the difference of the absolute contributions compared to PD (e.g. SSP2-4.5 minus PD)

## S12 References

### References

- Hoor, P., Borken-Kleefeld, J., Caro, D., Dessens, O., Endresen, O., Gauss, M., Grewe, V., Hauglustaine, D., Isaksen, I. S. A., Jöckel, P., Lelieveld, J., Myhre, G., Meijer, E., Olivie, D., Prather, M., Schnadt Poberaj, C., Shine, K. P., Staehelin, J., Tang, Q., van Aardenne, J., van Velthoven, P., and Sausen, R.: The impact of traffic emissions on atmospheric ozone and OH: results from QUANTIFY, *Atmos. Chem. Phys.*, 9, 3113–3136, doi:10.5194/acp-9-3113-2009, URL <http://www.atmos-chem-phys.net/9/3113/2009/>, 2009.
- Jöckel, P., Tost, H., Pozzer, A., Kunze, M., Kirner, O., Brenninkmeijer, C. A. M., Brinkop, S., Cai, D. S., Dyroff, C., Eckstein, J., Frank, F., Garny, H., Gottschaldt, K.-D., Graf, P., Grewe, V., Kerkweg, A., Kern, B., Matthes, S., Mertens, M., Meul, S., Neumaier, M., Nützel, M., Oberländer-Hayn, S., Ruhnke, R., Runde, T., Sander, R., Scharffe, D., and Zahn, A.: Earth System Chemistry integrated Modelling (ESCiMo) with the Modular Earth Submodel System (MESSy) version 2.51, *Geosci. Model Dev.*, 9, 1153–1200, doi:10.5194/gmd-9-1153-2016, URL <http://www.geosci-model-dev.net/9/1153/2016/>, 2016.